Synthesis of nanosized $BaCeO_3$ from oxalate precursor

Udayraj C. Yadav, Yuvraj S. Malghe*

Department of Chemistry, The Institute of Science, 15, Madam Cama Road, Mumbai 400032, India

*Corresponding author, Tel: (+91) 22-22844219; Fax: (+91) 22-22816750; E-mail: ymalghe@yahoo.com

Received: 31 March 2016, Revised: 04 October 2016 and Accepted: 01 November 2016

DOI: 10.5185/amp.2017/854
www.vbripress.com/amp

Abstract

Nanosized barium cerate ($BaCeO_3$) was prepared from barium cerium oxalate (BCO) precursor. Thermal decomposition of BCO precursor was studied using thermogravimetry(TG), differential thermal analysis (DTA), Fourier transform infrared spectroscopy (FTIR) and X-ray diffraction (XRD) techniques. BCO precursor calcined at 1000°C for 2h gives nanosized $BaCeO_3$ powder. Band gap of $BaCeO_3$ was estimated using diffuse reflectance spectrophotometry and is found to be 2.17 eV. Particle size distribution study reveals that particle size of $BaCeO_3$varies between 10-70 nm. Dielectric behavior of $BaCeO_3$ was studied with varying the temperature at different frequencies. $BaCeO_3$ shows good dielectric and conductivity response.

Keywords: $BaCeO_3$, precursor, dielectric material, impedance, conductivity.

Introduction

In recent years perovskite type ceramic materials such as $BaCeO_3$ have received considerable attention due to their electrical properties [**1**], photo catalytic activity [**2**], hydrogen gas and humidity sensing [**3**], electrolyte material for solid oxide fuel cell [**4,5**] and its high temperature conductivity. Dy doped $BaCeO_3$ shows better conductivity than Y doped [**5**] $BaCeO_3$. $BaCeO_3$ show better proton conductivity but have less mechanical and chemical stability, so it is doped with Zr in order to increase its stability and conductivity [**6**]. The melting point of $BaCeO_3$ is 1480°C [**7**] so sintering of this material must be done below this temperature. $BaCeO_3$ exhibits numerous applications in various fields. It is semiconductor type ceramic material and used as a sensor. Ti doped $BaCeO_3$ can be used as an electrolyte for capacitor application. Gd doped $BaCeO_3$ find application as a proton conducting membrane for hydrogen separation and used as a membrane in a reactor [**8**]. $BaCeO_3$ exhibit moderate densification property [**9**] but for capacitor application material must have high density. The densification can be achieved by using fine powder and adding additives during sintering. $BaCeO_3$ in cubic phase can be used as high temperature semiconductor [**10**]. Different methods such as Pechini method [**2**], sol-gel method [**6, 7, 11**], hydrothermal synthesis [**3**] etc. are used for the preparation of $BaCeO_3$. In present work nanosized $BaCeO_3$ was synthesized using oxalate co-precipitation method. This method is having several advantages over other existing methods. Homogeneous mixing of reactants gives the homogeneous product, also the method is simple, easy, cost effective and it gives product at low temperature. This is the simple and direct process for the synthesis of fine metal oxide powders, which are highly reactive and shows better sinterability. Hence in the present work nanosized $BaCeO_3$ powder was prepared from BCO precursor. The electrical properties (dielectric and conductivity) of $BaCeO_3$ synthesized in the present work are investigated using impedance analyzer. It is observed that dielectric properties of material varies with temperature and frequencies. It shows better conductivity at 500°C.

Experimental

Materials used for preparation of barium cerium oxalate (BCO) precursor

Barium nitrate ($Ba(NO_3)_3$) purity 99.5%, cerium nitrate ($Ce(NO_3)_3.6H_2O$) purity 99.0% and ammonium oxalate ($(NH_4)_2C_2O_4.H_2O$) purity 99.0% were used for the preparation of barium cerium oxalate (BCO) precursor. All the chemicals used for the synthesis are Analytical reagent (AR) grade and procured from S.D. Fine Chemicals Ltd. (Mumbai, India).

Preparation of barium cerium oxalate (BCO) precursor

Aqueous solution of barium nitrate was prepared by dissolving 6.53g $Ba(NO_3)_3$ in 100cm^3 of distilled water. pH of this solution was ~6.73. Aqueous solution of cerium nitrate having pH ~3.56 was prepared by dissolving 10.86g$Ce(NO_3)_3.6H_2O$ in 100cm^3 distilled water. Ammonium oxalate solution (having pH ~ 6.22) was prepared by dissolving 7.11g $(NH_4)_2C_2O_4.H_2O$ in 100cm^3 distilled water. All these solutions were heated to

boil. Initially hot aqueous solution of barium and cerium nitrate were mixed together and stirred to obtain clear solution having pH ~ 4.42. To this mixture hot ammonium oxalate solution was added with a constant stirring to get white precipitate. Little excess ammonium oxalate solution was added to the mixture to ensure complete precipitation. pH of the precipitate was measured and found to be ~5.00. The precipitate was filtered. The white residue obtained was washed initially with distilled water and finally with acetone and then dried in an oven at 40°C for 24h. The product thus obtained was analyzed and assigned the formula [$BaCeO(C_2O_4)_2.4H_2O$].

Thermogravimetry (TG) and differential thermal analysis (DTA) study

BCO precursor was analyzed using TG and DTA system (Rigaku, Model- Thermo Plus TG8120). For recording TG and DTA curves 10.9 mg sample was heated in a nitrogen atmosphere with a constant heating rate 10°C min^{-1}. Alumina is used as a reference material for recording DTA curve.

Synthesis of $BaCeO_3$

BCO precursor was calcined in muffle furnace in the temperature range 800 to 1000°C for 2h with an interval of 100°C. The calcined powders were analyzed using X-ray diffractometer (Rigaku, Model-Miniflex II) using CuKα x-ray radiation having wavelength 0.15405nm. BCO precursor and precursor calcined at various temperatures were analysed using FTIR spectrophotometer (Perkin Elmer, Model- Spectrum 100). SEM images of $BaCeO_3$ were recorded using scanning electron microscope (SEM) (SEI, Model- Quanta 200 ESEM). Particle size of $BaCeO_3$ was measured using transmission electron microscope (TEM) (FEI, USA, Model-Technai-G2). Particle size distribution of $BaCeO_3$ was studied using particle size analyzer (Nanosight, Model-NTA-LM-20). Diffuse Reflectance spectroscopic study was carried out using UV-visible spectrophotometer equipped with diffuse reflectance accessory (Schimadzu, Model-UV-1800). Dielectric properties of $BaCeO_3$ pellet sintered at 1300°C were investigated using impedance analyzer (Wayne Kerr, Model-6500B).

Results and discussion

TG and DTA study of BCO precursor

TG and DTA curves of BCO precursor were recorded in nitrogen atmosphere and are presented in **Fig. 1(a).** TG curve show that BCO precursor decomposes through four steps. In the first step, in temperature range 25-125°C, mass loss is due to loss of one water molecule. It is followed by the second step (in temperature range 126-300°C) in which mass loss is due to loss of three water molecules. Mass losses observed in the third and fourth steps are due to decarboxylation. The observed and expected mass losses of BCO precursor are shown in **Table 1.**

Table 1. TG data of dried BCO precursor.

Steps	Temperature range/°C	Expected mass loss/%	Observed mass loss/%
I	RT-125	3.33	2.92
II	126-300	9.97	8.31
III	301-625	18.50	23.81
IV	626-900	8.13	6.08
Total mass loss/%		39.93	41.12

DTA curve show four endothermic peaks and two small exothermic peaks. First three endothermic peaks are due to loss of water molecule, while endothermic peak near 400°C is due to the decomposition of carboxylate group [**12, 13**]. The exothermic peak near 700°C is due to loss of CO and CO_2 molecules, other exothermic peak near 850°C is due to the formation of product $BaCeO_3$. From TG and DTA study thermal decomposition mechanism for the decomposition of BCO precursor is proposed as follow.

$$BaCeO(C_2O_4)_2.4H_2O \longrightarrow BaCeO(C_2O_4)_2.3H_2O + H_2O$$
$$BaCeO(C_2O_4)_2.H_2O \longrightarrow BaCeO(C_2O_4)_2 + 3H_2O$$
$$2BaCeO(C_2O_4)_2 \longrightarrow BaCeO_3 + BaCO_3 + CeO_2 + 4CO\uparrow + 3CO_2\uparrow$$
$$BaCO_3 + CeO_2 \longrightarrow BaCeO_3 + CO_2\uparrow$$

The information obtained from TG and DTA study of BCO precursor was used to select the calcination temperature to obtain final product, $BaCeO_3$.

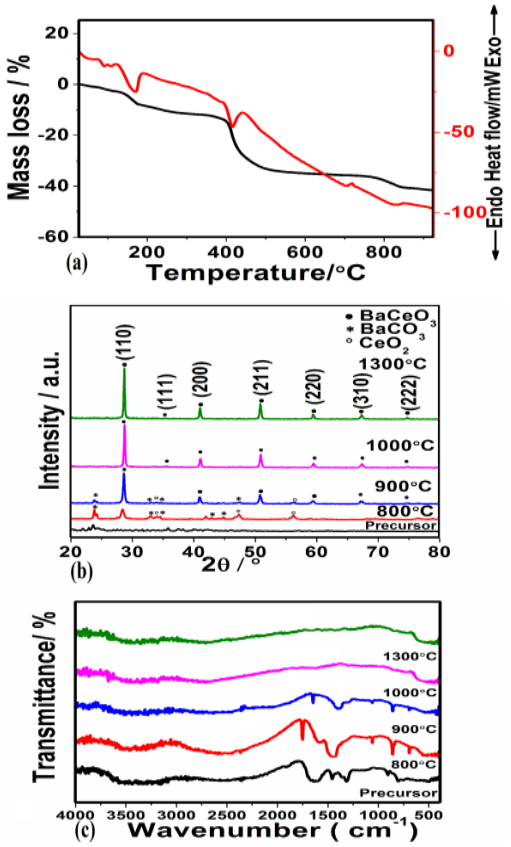

Fig. 1. (a) TG and DTA curves of BCO precursor, (b) XRD patterns of BCO precursor and precursor calcined at different temperatures, (c) FT-IR spectra of BCO precursor and precursor heated at different temperatures.

X-rays diffraction study

XRD patterns of BCO precursor and precursor calcined at various temperatures are shown in **Fig. 1 (b).** XRD pattern of precursor calcined at 800°C indicates that the product obtained at this temperature consist the mixture of $BaCeO_3$, $BaCO_3$ and CeO_2. Also the precursor calcined at 900°C consists $BaCO_3$ and CeO_2 as impurities but at this temperature the percentage of these impurities decreased. In the XRD pattern of the precursor calcinedat 1000°C the lines of $BaCO_3$ and $CeO_2$are absent suggesting that at this temperature pure $BaCeO_3$ phase is formed. XRD data indicate that $BaCeO_3$ prepared in the present work has cubic structure (JCPDS: 75-0431). XRD pattern of precursor calcined at high temperature (1300°C) shows increase in peak intensities indicating the increase in crystallinity of the product. Crystallite size of $BaCeO_3$prepared at 1000°C was calculated using Debye-Scherrer equation [14] and found to be is 51.20 nm.

IR study

IR spectra of BCO precursor and precursor heat treated at different temperatures were recorded and are presented in **Fig. 1(c).** IR spectra of BCO precursor shows absorption peaks at 1640, 1420, 1280, and 914 cm^{-1} represents oxalate vibration frequencies [**13, 14**]. Broad absorption band at 1700 and 3600 cm^{-1} indicate the presence of water molecule. Precursor heated at 800°C show carbonate vibration at 690, 870, 1060 and 1434 cm^{-1}[**15**] indicating the presence of $–CO_3$ group. The intensities of carbonate vibration peaks decrease at 900°C and these peaks disappears when sample is heated at1000°C for 2 h. Peaks around 1385 cm^{-1},503cm^{-1} and peaks between1500 to 1700 cm^{-1} are due to Ce-O vibration [**16, 3**]. Two strong absorption peaks near 1448 and858 cm^{-1} are due to $Ba-CO_3$vibration. Absorption peak at 558 cm^{-1} is due to Ce in octahedric coordination in the perovskite structure.

Scanning electron microscopy (SEM) study

SEM image of $BaCeO_3$ powder prepared at 1000°C is shown in **Fig. 2 (a).** It shows that the $BaCeO_3$ powder is heterogeneously distributed and having uneven morphology. SEM image of $BaCeO_3$ pellet sintered at 1300°C is presented in **Fig. 2 (b)**. This figure show that $BaCeO_3$ particles are having uneven distribution but the particles are well sintered and densely packed.

Transmission electron microscopy (TEM) and selected area electron diffraction (SAED) study

TEM image and SAED pattern of $BaCeO_3$ powder prepared at 1000°C are shown in **Fig. 2 (c).** The TEM image show that $BaCeO_3$ particles are polydispersed, nearly spherical in shape and particle size varies between 30 nm to 80 nm. This figure also shows that $BaCeO_3$ particles are agglomerated. Selected area electron diffraction (SAED) pattern indicates that $BaCeO_3$ prepared in this work is crystalline in nature.

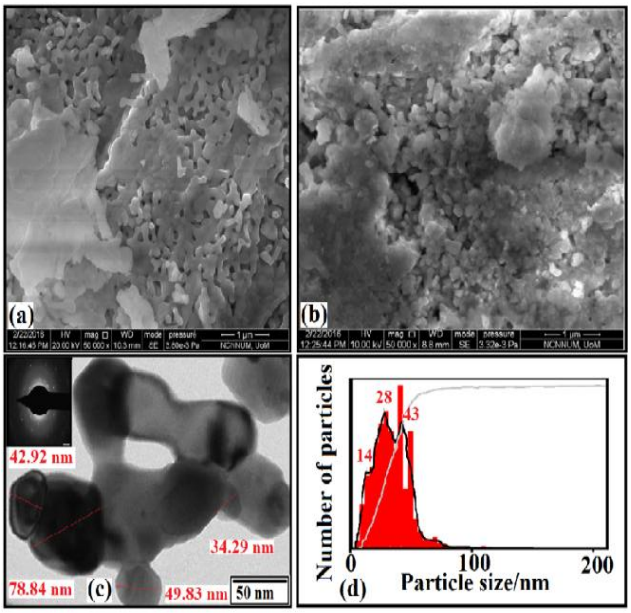

Fig. 2. (a) SEM image of $BaCeO_3$ powder prepared at 1000°C, (b) SEM image of $BaCeO_3$ pellet sintered at 1300°C. (c) TEM image and SAED pattern of $BaCeO_3$ powder (d) Particle size distribution curve of $BaCeO_3$ powder.

Particle size study

Particle size analysis study of $BaCeO_3$ powder was carried out using particle size analyzer and data obtained is shown in **Fig. 2 (d).** This figure reveals that the particle size of $BaCeO_3$varies between 10to70 nm and a maximum number of particles have particle size 43 nm.

Diffuse reflectance spectrophotometry study

The band gap of $BaCeO_3$ powder was estimated using modified Kubeka-Munk [**17**] relation followed by Tauc plot (plot of $(F(R).\ hv)^2$ versus photon energy) **Fig. 3.** Optical band gap for indirect allowed transition in $BaCeO_3$ was calculated and found to be 2.17 eV [**10**]. $BaCeO_3$ exhibit semiconductor property and cubic crystal system has a smaller band gap value compared to orthorhombic phase.

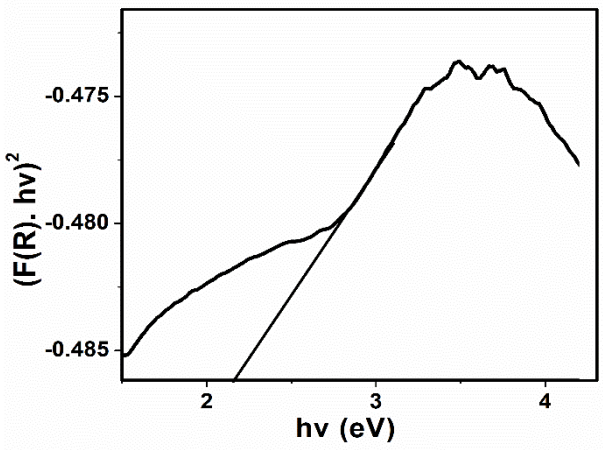

Fig. 3. Tauc plot $[(F(R).\ hv)^2$ versus photon energy (hv)] for $BaCeO_3$.

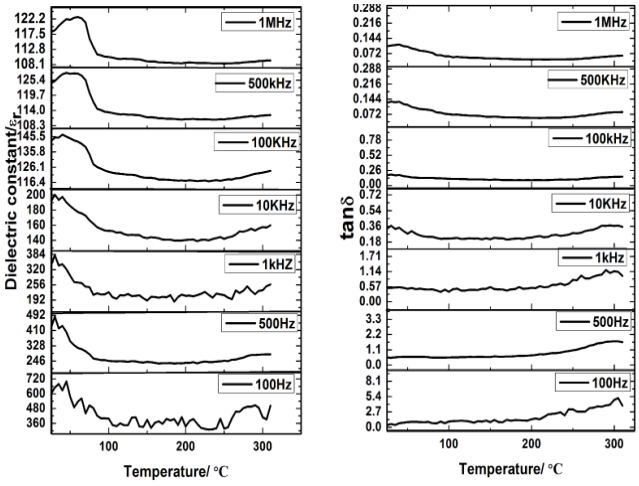

Fig. 4. (a) Plots of ε (dielectric constant) versus temperature for $BaCeO_3$ pellet sintered at 1300°C (b) Plots of tanδ versus temperature for $BaCeO_3$ pellet sintered at 1300°C.

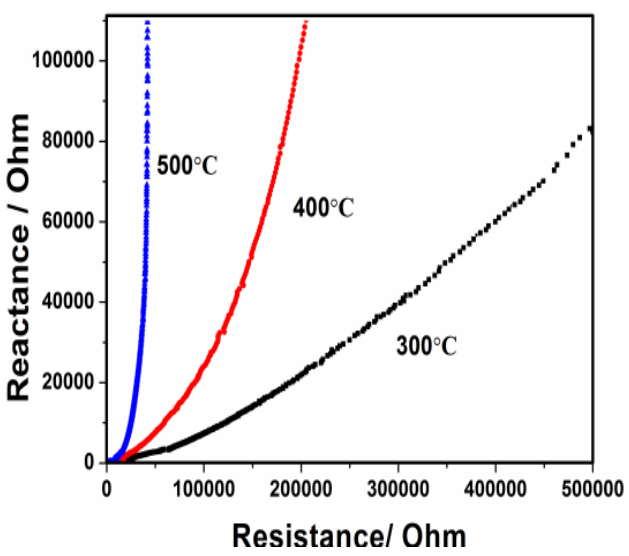

Fig. 5. Plot of reactance versus resistance at different temperatures for $BaCeO_3$ pellet sintered at 1300°C.

Study of dielectric properties

$BaCeO_3$ powder was pelletized using hydraulic press by applying 5ton pressure, and pellet was sintered at 1300°C for 3h. Dielectric constant and dielectric loss (tan δ) of sintered pellet were measured from room temperature to 310°C at different frequencies varying from 100Hz to 1MHz and shown in **Fig. 4 (a)** and **(b)** respectively. **Fig. 4 (a)** show that dielectric constant is inversely proportional to frequency. As frequency increases, dielectric constant decreases. Dielectric constant does not vary considerably with temperature. **Fig. 4 (b)** show that dielectric loss (tan δ) varies with frequency but dielectric loss of material is very low.

AC conductivity study

AC conductivity of $BaCeO_3$ prepared in present work is calculated using following relation [**18**]

$$\sigma ac = 2\pi\varepsilon_0\varepsilon_r f \tan\delta$$

where, ε_0 is permittivity of free space, ε_r is dielectric constant of material, f is applied field frequency and tan δ is dielectric loss of material. **Table 2** consists the calculated σac values obtained at different frequencies. The values of frequencies, dielectric constant and dielectric loss are estimated using **Fig. 4(a)** and **(b)**. This table indicate that dielectric constant varies with frequency. Its value is inversely proportional to frequency [**19**]. σac values are also vary with frequencies.

Table 2. Data of AC conductivity measurement.

Frequency	Dielectric constant	σac
100 Hz	606.11	3.57076 E-09
500 Hz	451.11	1.54192E-08
1 k Hz	349.144	3.12416E-08
10 k Hz	194.3	3.5852E-07
100 k Hz	142.72	8.40802E-07
500 k Hz	124.11	1.56925E-05
1M Hz	118.48	9.61393E-06

From impedance spectra shown in **Fig. 5,** it is observed that impedance curves for $BaCeO_3$ varies with temperature. It is observed that at 300°C resistance is more but at high temperatures (400 and 500°C) resistance decreases and conductivity of material increases. This is due to electron hole hopping mechanism which causes polarization and conduction as in case of small polarons [**18, 19, 20**]. It is also observed that with increase in frequency the conductivity of material increases. In temperature range 300-500^{0}C $BaCeO_3$ gives Nyquist type of impedance plots as shown in **Fig. 5.**

Conclusion

Nanosized $BaCeO_3$ powder was successfully prepared from BCO precursor at 1000 °C within 2 h. XRD data indicates that $BaCeO_3$ prepared in the present work is having a cubic structure. The particle size study show that particle size varies between 10nm to 70nm. SEM and TEM study shows that $BaCeO_3$ particles are heterogeneously distributed. Band gap of $BaCeO_3$ prepared in this work is 2.17 eV. Dielectric constant of $BaCeO_3$ decreases with increase in frequency. The method used for the synthesis of nanosized $BaCeO_3$ is easy, simple and cost effective. Conductivity study of $BaCeO_3$ show that conductivity increases with temperature. Materials dielectric and conductivity properties can be used for high temperature electrical application.

Acknowledgements

Authors are thankful to UGC, New Delhi for financial assistance. Authors are thankful to Sophisticated Analytical Instrumentation Facility, I.I.T., Mumbai for recording TEM images of the sample and National Centre for Nanoscience and Nanotechnology, University of Mumbai, Mumbai for recording SEM images of the sample.

Author's contributions

UC - Performed the experiments, YS - Data analysis, Wrote the paper. Authors have no competing financial interests.

References

1. Chen, F.; Wang, P.; Sorensen, T.; Menga, G.; Penga, D; J. Mater. Chem., 1997, 7, 1533. **DOI:** 10.1039/A608289K
2. Yuan, Y.; Zheng, J.; Zhang, X.; Li, Z.; Yua, T.; Ye, J.; Zou, Z; J. Solid StateIonics, 2008, 178, 1711. **DOI:** 10.1016/j.ssi.2007.11.012
3. Chao**,** X.**;** Junwu, Z.; Xujie**,**Y.; Lude, L.; Xin, W; J. Rare Earths, 2008, 26, 51. **DOI:** 10.1016/S1002-0721(08)60036-8
4. Lin, H.; Chiang, R.;Kuo, C.; Chang, C; J. Non-Crystalline Solids, 2007, 353, 1188. **DOI:** 10.1016/j.jnoncrysol.2006.09.042
5. Lyagaeva, J.; Danilov, N.; Vdovin, G.; Bu, J.; Medvedev, D.; Anatoly, D.; Tsiakaras, P; *J. Mater. Chem*. A, 2016, 00, 1. **DOI:** 10.1039/C6TA06414K
6. Osman, N.; Ibarahim, N. A;Ishak, M.A.A.; Hasaan, O.H; Sains Malaysiana, 2014, 43, 9, 1373.
7. Koferstei, R.; Hesse, D.; Ebbinghaus, S;J. Solid State Ionics, 2011, 203, 52. **DOI:** 10.1016/j.ssi.2011.09.010
8. Zając, W.; Rusinek, D.; Zheng, K.; Molenda, J;Cent. Eur. J. Chem., 2013, 11, 471. **DOI:** 10.2478/s11532-012-0144-9
9. Koferstein, R.; Jager, L.; Ebbinghaus, S; J. Mater. Sci., 2010, 45, 6521. **DOI:** 10.1007/s10853-010-4741-8
10. Aycibin, M.; Erdinc, B.; Akkusi, H; J. Electr. Mater., 2014, 43, 4301. **DOI:** 10.1007/s11664-014-3378-9
11. Chokkha, S.; Kuharuangrong, S; J. Metals Materials Minerals, 2010, 20, 55.
12. Malghe,Y; J. Therm. Anal. Calorim., 2010, 102,831. **DOI:** 10.1007/s10973-010-0786-9
13. Lavand, A.; Malghe,Y; J, Therm. Anal. Calorim., 2014, 118,1613. **DOI:** 10.1007/s10973-014-4033-7
14. Elbaccouch, M.;Shukla, S.; Mohajeri, N.; Seal, S.;T-Raissi, A; J. Solid State Ionics, 2007, 178, 19. **DOI:** 10.1016/j.ssi.2006.10.026
15. Rij, L.; Winnubst, L.; Jun, L.; Schoonman, J; J. Mater. Chem., 2000, 10, 2515. **DOI:** 10.1039/b003840g
16. Singh, J.;Ketzial, J.; Radhika, D.;Nesaraj, A; Ketzial et al. Int. J. Ind. Chem., 2013, 4, 18. **DOI:** 10.1186/2228-5547-4-18
17. Lopez, R.; Gomez, R; J. Sol-Gel Sci. Technol. 2012, 61, 1. **DOI:** 10.1007/s10971-011-2582-9
18. Khetre, S.; Jadhav, H.; Jagadale, P.; Kulal, S.; Bamane, S;Adv. Appl. Sci. Res., 2011, 2, 503.
19. Patil, D.;Chougule, B; J. of All. Comp., 2009, 470, 531. **DOI:** 10.1016/j.jallcom.2008.03.006
20. Ouzaouit, K.; Benlhachemi, A.; Benyaich, H; M. J. Cond. Mater., 2006, 7, 11.
21. Medvedev, D.; Maragou, V.; Zhuravleva, T.; Demin, A.; Gorbova, E.; Tsiakaras, P; J. Solid State Ionics, 2011, 182, 41. **DOI:** 10.1016/j.ssi.2010.11.008
22. Gorbova, E.; Maragou, V.; Medvedev, V.; Demin, A.; Tsiakaras, P; J. Solid State Ionics, 2008, 179, 887. **DOI:** 10.1016/j.ssi.2008.02.065
23. Chena, Q.; Braun, A.; Yoon, S.;Bagdassarov, N.;Graule, T; J. Europ. Cer. Soc., 2011, 31, 2657. **DOI:** 10.1016/j.jeurceramsoc.2011.02.014
24. Tan, X.;Songb, J.; Mengb, X.; Mengb, B.; J. Europ. Cer. Soc., 2012, 32, 2351 **DOI:** 10.1016/j.jeurceramsoc.2012.03.004
25. Matskevich, N.; Wolf, T.; Matskevich, M.; Chupakhina, T; Eur. J. Inorg. Chem. 2009, 11, 1477. **DOI:** 10.1002/ejic.200800589
26. Orlov, A.; Shlyakhtin, O.;Vinokurov, A.;Knotko, A.; Tretyakov, Y; J.Inorg., Mater., 2005,41, 1194. **DOI:** 10.1007/s10789-005-0286-7
27. Lee, D.; Won, J.; Shim, K; Materials Letters, 2003, 57, 3346. **DOI:** 10.1016/S0167-577X(03)00072-7

